Implementation of Optical Meanders of the Optical-Fiber DTS System Based on Raman Stimulated Scattering into the Building Processes

Petr KOUDELKA[1], Jan LATAL[1], Jan VITASEK[1], Jan HURTA[2], Petr SISKA[1], Andrej LINER[1], Martin PAPES[1]

[1]Department of Telecommunications, Faculty of Electrical Engineering and Computer Science, VSB-Technical University of Ostrava, 17. listopadu 15, 708 33 Ostrava-Poruba, Czech Republic

[2]Laboratory of Building Materials, Faculty of Civil Engineering, VSB-Technical University of Ostrava, Ludvika Podeste 1875/17, 708 33 Ostrava-Poruba, Czech Republic

petr.koudelka@vsb.cz, jan.latal@vsb.cz, jan.vitasek@vsb.cz, jan.hurta@vsb.cz, petr.siska@vsb.cz, andrej.liner@vsb.cz, martin.papes@vsb.cz

Abstract. *The Optical fiber DTS (Distribution Temperature Systems) are unique distributed temperature systems using optical fiber as a sensor. These systems are able to measure the temperature along the fiber, in some case they can measure tension as well. For their function they use nonlinear effect in optical fiber (Raman nonlinear effect, Brillouin nonlinear effect). The greatest advantage of this sensor system is just using of the optical fiber (electromagnetic resistance, small size, safety using in inflammable and explosive area, easy installation, etc.). The Optical fiber DTS systems can be used with advantage even in areas, where the using of classic sensors would be problematic. The typical example is monitoring of outflows in pipelines, illegal service connection etc. In some processes it is necessary to know the exact temperature (tension) in particular points. There it can appear a problem with resolution of the optical-fiber DTS. This article deals with problems of the optical meanders implementation into the building processes.*

Keywords

Heat of hydration, concrete, optical-fiber DTS, optical meanders, Raman stimulated scattering, sensory ring.

1. Introduction

The optical fiber DTS (*Distribution Temperature Systems*) are unique distributed temperature systems using optical fiber as a sensor. Due to advantageous features of optical fiber these sensory systems begin to be utilizing in industry [1]. In some cases optical fiber DTS is indispensable helper today:

- monitoring of outflow from oil pipeline,
- monitoring of outflow from product pipeline,
- monitoring of water percolatin from hydraulic structure,
- temperature profile measurement of borehole in rock pillar (heat pumps).

The optical fiber DTS uses nonlinear effects in optical fiber, Raman or Brillouin nonlinear effect respectively. Optical-Fiber DTS using Brillouin stimulated scattering is able to measure temperature and tension along an optical fiber in distance of 50 km, nevertheless due to higher purchase cost the industry rather uses systems based on Raman nonlinear effect.

Technologically, the optical fiber DTS is based on optical reflectometer principle. In the optical fiber a light pulse is transmitted with wavelength of 975 nm, 1064 nm or 1550 nm (in dependence on construction of DTS) and with width of 10 ns.

2. Optical-Fiber DTS Based on Raman Stimulated Scattering

The physical principle of optical-fiber DTS comes out from the description of Raman stimulated scattering.

2.1. Raman Stimulated Scattering

The simplest description of Raman stimulated scattering is a quantum mechanical model. Except quantum mechanical model of Raman scattering there is

description based on induction of the dipole moment in the molecule by the instrumentality of oscillating the electric field of exciting radiation. This induced dipole μ_i is then a source of scattering radiation and it is directly proportional to electric field intensity E:

$$\mu_i = \alpha \cdot E. \tag{1}$$

The proportion coefficient α is called electric polarizability coefficient. It sets how much it is possible to change a charge patterns. This coefficient means efficiency with which the acting AC electric field is able to induce a dipole moment in molecule. Because the vector μ_i has other direction than vector E, the electric polarizability can't be a scalar but it is a tensor represented by symmetric matrix [2]:

$$\alpha_{ij} = \begin{pmatrix} \alpha_{xx} & \alpha_{xy} & \alpha_{xz} \\ \alpha_{yx} & \alpha_{yy} & \alpha_{yz} \\ \alpha_{zx} & \alpha_{zy} & \alpha_{zz} \end{pmatrix}. \tag{2}$$

Relative motions of atoms by normal vibration mode cause changes of polarizability tensor in isotropic and anisotropic molecules. Instantaneous value of vibrations is set by relation:

$$r = R_0 \cos 2\pi v_{vib} t, \tag{3}$$

where R_0 is an amplitude of vibration with frequency v_{vib}. By neglecting of higher orders of polarizability tensor Taylor series and next adjustment we obtain the final relation of the dipole moment [3]:

$$\mu_i = \alpha_0 E_0 \cos(2\pi v_0 t) + \\ + \frac{1}{2}\left(\frac{\partial \alpha}{\partial r}\right)_0 R_0 E_0 \cos[2\pi(v_0 - v_{vib})t] + \\ + \frac{1}{2}\left(\frac{\partial \alpha}{\partial r}\right)_0 R_0 E_0 \cos[2\pi(v_0 + v_{vib})t]. \tag{4}$$

In Eq. (4) there are three terms with a different value of frequency of scattering radiation. For correct understanding of Raman-DTS behavior are important the second and the third terms of equation. These terms correspond to Stokes and anti-Stokes part of Raman scattering. Stokes part is characterized by lower frequency than frequency of excitation radiation, anti-Stokes part is characterized by higher frequency (Fig. 1).
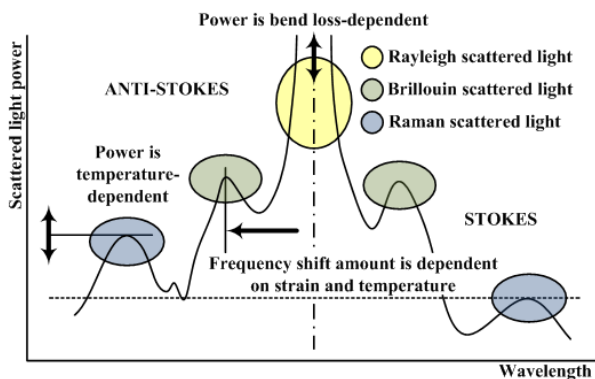

Fig. 1: Spectrum of the backscattered light of optical fiber.

From Eq. (4) is obvious:

$$\frac{\partial \alpha}{\partial r} \ll \alpha_0, \tag{5}$$

therefore the Raman scattering intensity is much lower than Rayleigh scattering intensity (Fig. 1). For the creation of anti-Stokes part it is necessary that the molecule would be in higher vibration energetic state at the beginning of this process. The population of higher vibration states is set by Boltzmann distribution, therefore the number of molecules in this state is small [2]. This corresponds to lower anti-Stokes intensity in comparison to Stokes intensity (Fig. 1):

$$\frac{N_1}{N_0} = e^{-\frac{h v_{vib}}{kT}}, \tag{6}$$

where N_0 is population in basic energetic state, N_1 is population in higher energetic state, h is Planck constant, v_{vib} is vibration frequency of molecule, k is Boltzmann constant and T is temperature.

2.2. Working Principle of Optical-Fiber DTS Based on Raman Stimulated Scattering

In the case when we want to measure temperature in a specific part of optical fiber z (distance from the forehead of optical fiber), it is necessary to aim for the spectrum of Raman scattering. I_S represents the Stokes intensity part of Raman scattering, I_{AS} represents the anti-Stokes intensity part of Raman scattering. The relations describing these intensities are written below (7), (8). For both relations it is valid the same relation for attenuation from forehead to position z, the lasers usually used in the optical-fiber DTS have a wavelength at 1064 nm. Peaks of Raman spectrum are in this case shifted $\pm$ 40 nm, i. e. 1104 nm and 1024 nm. Due to the fact, that the attenuation is a function of wavelength, this effect can cause an error in temperature determination [4].

$$I_S(z) = C_S e^{-\alpha_R z} e^{-\alpha_S z} \langle n_k \rangle, \tag{7}$$

$$I_{AS}(z) = C_{AS} e^{-\alpha_R z} e^{-\alpha_{AS} z} (\langle n_k \rangle + 1), \tag{8}$$

where C_S and C_{AS} are constants and

$$\langle n_k \rangle = \frac{e^{-\frac{\hbar\Omega}{kT(z)}}}{1 - e^{-\frac{\hbar\Omega}{kT(z)}}}, \tag{9}$$

where $\hbar$ is reduced Planck constant, k is Boltzmann constant, $2\pi\Omega$ is red and blue shift in frequency. It is a valid approximation relation:

$$\frac{\hbar\Omega}{k} \cong 600\,{}^\circ K. \tag{10}$$

For the optical fiber distributed systems, which are using the Raman stimulated scattering for their function,

the anti-Stokes part of the spectrum is the most important. This part of spectrum changes the intensity in dependence on temperature change along an optical fiber (Fig. 1). Stokes part of spectrum embodies temperature independence. The DTS systems therefore principally work on the basis of the anti-Stokes part intensity to the Stokes part intensity ratio [5]:

$$\frac{I_S(z)}{I_{AS}(z)} = \frac{C_S}{C_{AS}} e^{-\Delta\alpha z} e^{-\frac{\hbar\Omega}{kT(z)}}, \qquad (11)$$

where $\Delta\alpha = \alpha_S - \alpha_{AS}$ is greater than zero. For laser wavelength at 1064 nm these differential losses embody value 0,347 dB/km. By solution relation (11) we obtain equation for temperature $T(z)$ in distance z in the form:

$$T(z) = \frac{\frac{\hbar\Omega}{kT(z)}}{\ln\left(\frac{C_S}{C_{AS}}\right) - \Delta\alpha z - \ln\left(\frac{I_S(z)}{I_{AS}(z)}\right)}. \qquad (12)$$

Equation (12) can be further written with the aid of power series with approximation

$$\frac{1}{(1-x)} = 1 + x + x^2 + \dots, \qquad (13)$$

on condition, that x takes small values and hence higher orders x can be irrelevant:

$$T(z) \cong \frac{\frac{\hbar\Omega}{k}}{\ln\left(\frac{C_S}{C_{AS}}\right) - \ln\left(\frac{I_S(z)}{I_{AS}(z)}\right)} \cdot$$

$$\cdot \left\{ 1 + \frac{\Delta\alpha z}{\ln\left(\frac{C_S}{C_{AS}}\right) - \ln\left(\frac{I_S(z)}{I_{AS}(z)}\right)} \right\}. \qquad (14)$$

By the adjustment of Eq. (14) we obtain the final mathematical relation describing function principle of the optical fiber DTS system on the basis of the Raman stimulated scattering (15). This equation is a linear combination of temperature offset (first part of the equation), difference of attenuation in optical fiber (second part of the equation) and temperature measurement on the basis of the anti-Stokes to the Stokes ratio (third part of equation):

$$T(z) \cong T_{REF} \left(1 + \frac{\Delta\alpha z}{\ln\left(\frac{C_S}{C_{AS}}\right)} + \frac{\ln\left(\frac{I_S(z)}{I_{AS}(z)}\right)}{\ln\left(\frac{C_S}{C_{AS}}\right)} \right), \qquad (15)$$

where for temperature offset T_{REF} the relation is valid:

$$T_{REF} = \frac{\hbar\Omega}{k \ln\left(\frac{C_S}{C_{AS}}\right)}. \qquad (16)$$

3. Optical-Fiber DTS Application into Civil Engineering

Today the concrete is the one of the most widely used construction material, its great advantage in terms of building constructions is its universality in use, good mechanical features in the pressure and possible connection with steel. The concrete is fine-ground inorganic material, which works like hydraulic binder. After mixture with water it makes concrete paste, which lastly stiffens and hardens. After hardening it retains its strength even in the water. This processes hardening and conversion of cinder minerals into concrete stone are called concrete hydration by which so called heat of hydration is released.

3.1. Hydration of Concrete Binder

The hydration of concrete binder is an exothermic reaction. The hydration of concrete happens after cinder is a mixture with water. During this process are gradually raised fine crystals and proportional couplings in the concrete mixture and heat is released. Intensity of hydration heat is proportional to reaction speed in dependence on the chemical-mineralogical structure of concrete, presence of active additives and ambient conditions. The total value of hydration heat of fully hydrated concrete is the sum of hydration heats of particular cinder minerals, which values (on 1 kg) are considerably different (Tab. 1).

The hydration of concrete binder can be divided in three phases. Each of them is characterized by specific degree of heat, time duration and reactions.

The first phase is often called inductive phase and takes approximately from 1 to 2 hours after cinder is mixture with water. This phase is divided into two parts. The first (preinductive) part is very short, it takes approximately 10-15 minutes and it is the process of wetting of concrete granules. The other part of inductive phase (dormant) does not release so much heat like the first part. There begins increasing of concrete paste viscosity, its state is close to viscous liquid [6].

Tab.1: Heat of hydration of cinder minerals [7].

Cinder mineral	Limiting value [kJ.kg^{-1}]
C_3A	800-1280
C_3S	380-540
C_4AF	120-440
C_2S	90-110
CaO	1116
MgO	812

The second phase of hydration (acceleration) takes approximately from 12 to 24 hours after cinder is a mixture with water. Thanks to hydration, especially C_3S, this phase is characteristic by the most expressive development of hydration heat and after that the concrete paste is in solid form with strength in the pressure about 20 MPa [6].

The third phase of hydration (deceleration) can take several years and it can be divided in into two parts as well. In other part, roughly after 28 days, the concrete paste begins to ripen, which is characterized by phases re-crystallization in space between concrete granules [7].

3.2. Present Methods of Determination of Hydration Heat

There are two basic methods, which can determinate the hydration heat for silicate binder:

- direct methods: monitoring temperature changes of sample with exact defined boundary condition,

- indirect methods: determination of hydration heat from heat of dilution of hydrated samples in acid mixture.

Indirect methods are relatively very accurate, but they are only able to determine the total value of heat of hydration in a specific state of hydration. By the help of indirect methods we dynamically monitor values, which are directly proportional to the intensity of hydration heat. The total value of released hydration heat we can determinate by integration this intensity [7].

3.3. Method of hydration heat determining using fiber optic DTS

The above mentioned current methods are applied only to samples of cement (silicate) binders. Fiber optic DTS allow application directly to the real constructions and then monitor the entire structure, not just the sample. Practically depends only on the requirement to which extent we want to know the temperature profile of measured masses of cement binder. This requirement is then equal to created fiber meander and number of layers. Due to practical experience in developing of fiber meander it appears to be most ideal a reinforced concrete structures [1].

Thanks to the sensor size, the optical fiber in this case (depending on the degree of protection of the fiber), and the price, seems to be this method very efficient. Furthermore, because of the method itself, which utilizing the nonlinear Raman (Brillouin) phenomenon in optical fibers, this method is very accurate. The method using fiber optic DTS can be described as a method which combines features of both direct and indirect methods - high accuracy and the ability to monitor the dynamics of values involved in the evolution of hydration heat [1].

4. Experimental Attestation of Method of Determination of Hydration Heat with using DTS

In the Laboratory of Building Materials, VSB-Technical University of Ostrava, it was performed experimental verification, which should confirm pertinence of this system for hydration temperature measurement in the concrete mixture. For higher hydration temperature of concrete mixture it was chosen girder with greater sizes 150×150×600 mm. The concrete mixture used in the manufacture of the measured test sample and the others comparative samples must allow for equal distribution of all ingredients inside concrete mixture even through optical fibers inserted into a mold (Fig. 2).
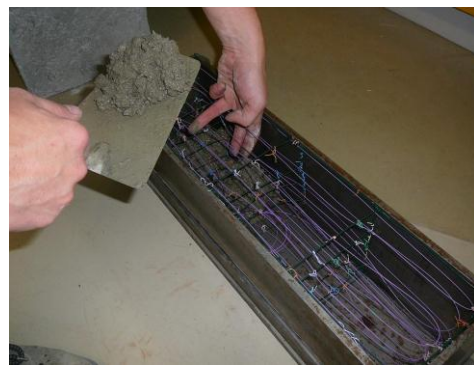

Fig. 2: Form filling by concrete mixture.

The determination of features of fresh concrete mixture was governed by standard CSN EN 206. For this mixture were done following tests:

- volume weight determination CSN EN 12350-6,

- air volume determination by method manometric vessel,

- consistence determination by slump cone CSN EN 12350-2 (transformation standardized Abrams cone),

- feature determination of nallous concrete proceeds in step with standard CNS EN 12390-3: determination of compressive strength for experimental solids after elapse of different time periods (keeping in water bath).

The volume weight ρ_0 is generally defined as the ratio of real sample weight m_0 to real volume of this sample V_0 (i. e. to volume including pits, cavities and scratches):

$$\rho_0 = \frac{m_0}{V_0}. \qquad (17)$$

The concrete mixture was mixed according to modified prescription for demands of better filling processing of fresh concrete mixture to fill in the whole space in the form with fiber meander system. The used prescription and fresh concrete features are written in

following tables (Tab. 1, Tab. 2 and Tab. 3).

Tab.2: Features of fresh concrete mixture.

Feature	Volume weight	Slump	Air volume
Result	2300 kg·m^{-3}	170 mm	2,2 %

Tab.3: Used prescription of concrete mixture.

Ingredients	Quantity
Concrete CEM I 42,5 R	320,0 kg·m^{-3}
Water	190,0 kg·m^{-3}
Aggregate *0-4 Tovacov*	850,0 kg·m^{-3}
Aggregate *4-8 Hrabuvka*	175,0 kg·m^{-3}
Aggregate *8-16 Hrabuvka*	765,0 kg·m^{-3}
Plasticizer FM 974	2,3 kg·m^{-3}

Tab.4: Strength features of harden concrete mixture.

Age	Sample	Area A_C	Force F	Strenght
3 days	H1	22210 mm^2	511,30 kN	23 MPa
7 days	H2	22623 mm^2	746,42 kN	33 MPa

The overall four layers of fiber meanders were created in the girder for experimental measurement, which were equally distributed in the form. The multimode optical fiber 50/125 µm with secondary PVC jacket was used. In case of fiber bending it wasn't broken a critical radius of fiber bending. During the experimental measurement wass found out that the critical radius of fiber bending is 35 mm with using DTS and multimode optical fiber 50/125 µm. If the radius is exceeded the measured results are devalued. The total length of 15 m of optical fiber was placed in the form. Figure 3 shows temperature behavior in a particular layers of fiber meander in the first period, i.e. 24 hours after placing of concrete mixture. The time change of temperature shows that in particular layers the different temperature risings occurred. In case of fiber meander that is placed more closely to bottom of form (Layer 4), the maximal temperature increases.
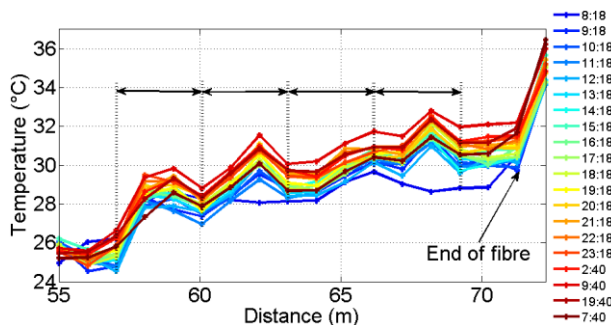

Fig. 3: Temperature behavior of hydration heat in first 24 hours after placing of concrete mixture.

At the beginning of the experiment the temperature was almost the same in all layers (average 28,2 °C). It is preinductive period - wetting of concrete granules (c. 15 min). For finding other phases of mixture hardening is necessary to set curves of the hydration heat. Overall there were set four curves of the hydration heat, respectively one for particular layer of fiber meanders.

From particular layers were chosen places on optical fiber, which correspond to the center of form (maximal values according to Fig. 3; 59 m, 62 m, 65 m and 68 m). The results in the time domain of the first three days are depicted on Fig. 4.
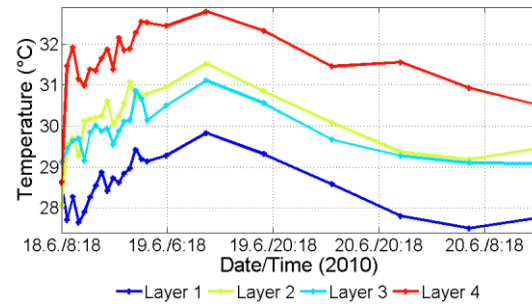

Fig. 4: Curves of hydration heat in particular layers of fiber meander in first three days.

From Fig. 4 is clearly visible the difference between the edge layers of fiber meander, which makes in its maximum 3 °C. It must be pointed out that this was an experimental measurement in metal form, which drains part of the heat. It can be supposed that in a real environment the difference will be far greater. During the experiment, the ambient temperature was constant at 25,5 °C.

5. Optical Meanders in Point Mode

In cases, when it is necessary to know the temperature in exactly determined places, the resolution of optical fiber DTS seems to be a big problem. The resolution of DTS is in the range from 1 to 2 m according to system configuration. The resolution of DTS is described by situation, when in the same part of optical fiber (z) the temperature grows up to 40 °C against ambient temperature 25 °C or 26 °C. In place with increased temperature ($z \pm$ resolution) the system is unable to localize other temperature change if it does not exceed mentioned temperature. The challenge of experimental measurement was to set the ideal size of sensory ring for optical fiber with primary coating (external diameter of 250 µm) and optical fiber with tight outer jacket (external diameter of 900 µm). The example of optical meander in point mode (matrix type) is shown on Fig. 5.
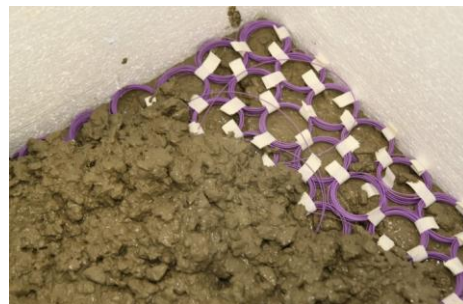

Fig. 5: The example of optical meander in point mode applied in civil engineering.

If it is necessary to know the exact localization it is suitable to apply the optical meanders in point mode. The point mode means that the sensory ring from optical fiber is created in the same place. The work experiences demand the smallest size of sensory ring (inner diameter and the length of optical fiber in ring). It is obvious that the size of sensory ring will change with different parameters of optical fiber [9].

The experimental measurement was done in Memmert water bath. The temperature of the water bath was kept at 40 °C ± 0,5 °C, the ambient temperature was 25 °C. The schematic diagram of experimental measurement is shown on Fig. 6.
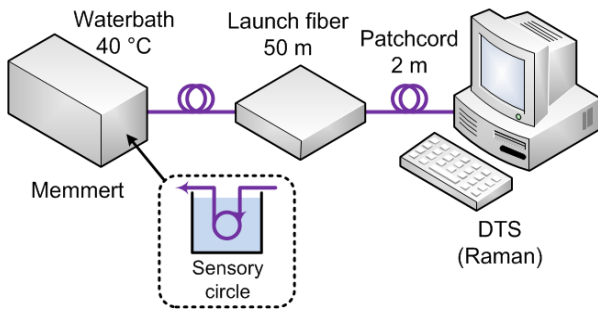
Fig. 6: The schematic diagram of experimental measurement.

The temperature in a water bath was controlled by lab mercury thermometer and digital thermometer Testo 720 with NTS probe, see Fig. 7.

Fig. 7: Temperature control of the water bath by lab mercury thermometer and digital thermometer Testo 720 with NTS probe.

5.1. Optical Fiber with Tight Outer Jacket (External Diameter 900 μm)

The first experimental measurement was meant to set the ideal size of sensory ring for optical meander in point mode. It was used multimode optical fiber with tight outer jacket (external diameter of 900 μm). The sensory rings with inner diameter in the range from 1,5 cm to 6 cm were created, each ring contained 5 m of optical fiber. The results of experimental measurement in a water bath are shown on Fig. 8.

Subsequently, all sensory rings were spliced together from the greatest inner diameter to the smallest inner diameter. The measured values are shown on Fig. 9.
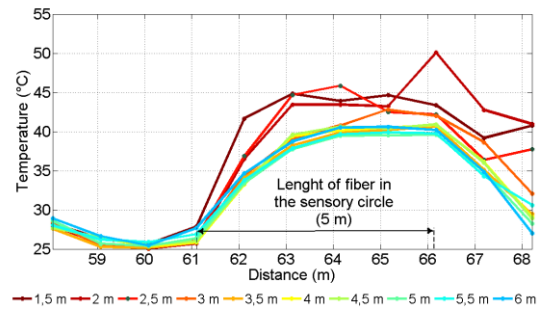

Fig. 8: Influence of inner diameter on measured temperature of the water bath (measured separately, optical fiber with tight outer jacket, external diameter of 900 μm).
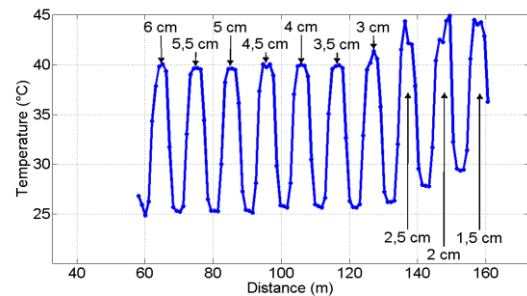

Fig. 9: Influence of inner diameter on measured temperature of the water bath (measured together, optical fiber with tight outer jacket, external diameter of 900 μm).

It is obvious from these results that the ideal inner diameter of sensory ring is 3,5 cm in case of optical fiber with tight outer jacket. If the inner diameter limit is overranged, the measured values are markedly biased.

The other experimental measurement was meant to set the ideal length of optical fiber in sensory ring. The procedure was similar. The sensory rings with fiber length from 1,5 m to 5 m were created, the inner diameter of sensory rings was chosen at 4 cm. The results of this experimental measurement in a water bath are shown on Fig. 10.
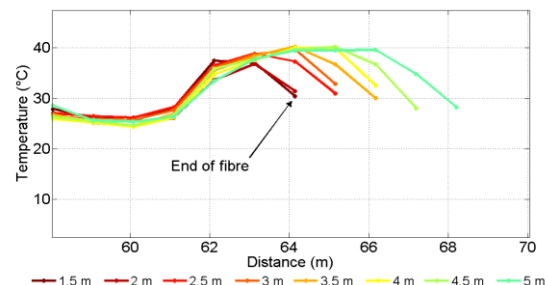

Fig. 10: Influence of fiber length in sensory ring on measured temperature of the water bath (measured separately, optical fiber with tight outer jacket, external diameter of 900 μm).

Subsequently, all sensory rings were spliced together from the longest length to the shortest length. The measured values are shown on Fig. 11.
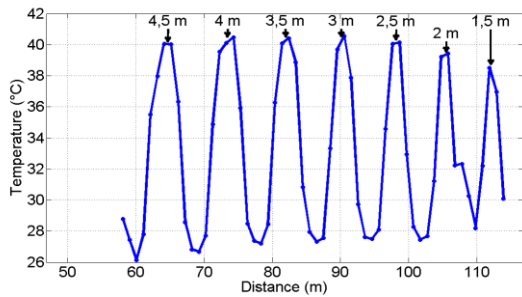
Fig. 11: Influence of fiber distance in sensory ring on measured temperature of the water bath (measured together, optical fiber with tight outer jacket, external diameter 900 µm).

From these results it can be clearly seen that the ideal length of optical fiber in sensory ring is 3 m in case of optical fiber with tight outer jacket. The measured values on Fig. 11 are not exact on level of 40 °C (40,5 °C). It is caused by inertia of Memmert in an endeavor to keep the temperature of the water bath on level 40 °C.

5.2. Optical Fiber with Primary Coating (External Diameter 250 µm)

The last experimental measurement was meant to set the ideal size of sensory ring for the multimode optical fiber with primary coating (external diameter 250 µm). The sensory rings with inner diameter from 1,5 cm to 6 cm were created, each ring contained 5 m of optical fiber. The results of experimental measurement in a water bath are shown on Fig. 12.

Subsequently, all sensory rings were spliced together from the greatest inner diameter to the smallest inner diameter. The measured values are shown on Fig. 13.

From these results is obvious that the ideal inner diameter of sensory ring is 3 cm in case of optical fiber with primary coating. The measured values shown on Fig. 12 and Fig. 13 are also not exact on level of 40 °C (41 °C). It was caused by inertia of Memmert in an endeavor to keep the temperature of the water bath on level 40 °C.
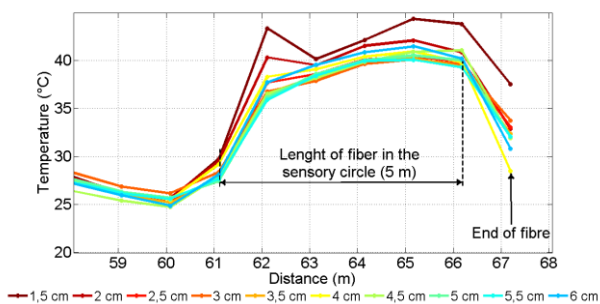

Fig. 12: Influence of inner diameter on measured temperature of the water bath (measured separately, optical fiber with primary coating, external diameter of 250 µm).
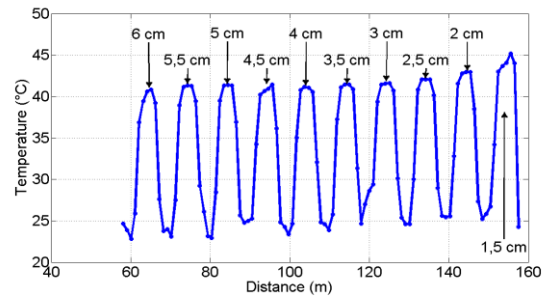

Fig. 13: Influence of fiber distance in sensory ring on measured temperature of the water bath (measured together, optical fiber with primary coating, external diameter of 250 µm).

6. Conclusion

The results of experimental measurements brought new findings from the field of implementation of optical meanders in civil engineering. The first part of this article is dealing with problems of using of classic optical meanders in civil engineering and analyzing of hydration heat in concrete binder.

The other part of the article deals with optical meanders in point mode. It is obvious from measured values that the ideal size of sensory rings from optical fiber with tight outer jacket (external diameter of 900 µm) is 3,5 cm (inner diameter) with fiber length of 3 m. In case of optical fiber with primary coating (external diameter of 250 µm), it is possible to reach smaller size of sensory ring about 3 cm of inner diameter.

The results of experimental measurements could be used not only in civil engineering, but also in monitoring of other industrial process, for example in temperature measurement of crystallizer.

Acknowledgements

References

[1] KOUDELKA, Petr, Bohumila PETRUJOVA, Jan LATAL, Frantisek HANACEK, Petr SISKA, Jan SKAPA and Vladimir VASINEK. Optical fiber distributed sensing system applied in cement concrete commixture research. *Radioengineering*. 2010, vol. 19, no. 1, pp. 172-177. ISSN 1210-2512.

[2] LONG, Derek. *The Raman Effect: A Unifield Treatment of the Theory od Raman Scattering by Molecules*. 1. ed. Chichester: John Willey & Sons, 2002. ISBN 978-0-471-49028-9.

[3] BALL, David W. Theory of Raman Spectroscopy. *Spectroscopy* [online]. 2001, vol. 16, no. 11, pp. 28-30. ISSN 0887-6703.

[4] RODERS, Alan. Distributed optical-fibre sensing. *Measurement Science and Technology* [online]. 1999, vol. 10, no. 8. ISSN 1361-6501. DOI:10.1088/0957-0233/10/8/201.

[5] JASKELAINEN, Mikko. Distributed Temperature Sensing (DTS) in Geothermal Energy Applications. *Spectroscopy* [online]. 2009, no. 9. ISSN 0746-9462.

[6] PYTLIK, Petr. *Technologie betonu*. Brno: VUTIUM, 2000. ISBN 80-214-1647-5.

[7] STASTNIK, Stanislav. Modelovani nestacionarniho 3D-teplotniho pole v zelezobetonovych konstrukcich. In: *Betonarske dny 2002*. Pardubice: CBS, 2002. ISBN 80-238-9644-X.

[8] CSN EN 12390-5. *Zkouseni ztvrdleho betonu - Cast 5: Pevnost v tahu ohybem zkusebnich tele*s. Brusel: Svaz vyrobcu betonu CR, IC 64935124, Februar 2009.

[9] SKAPA, Jan, Jan LATAL, Marek PENHAKER, Petr KOUDELKA, Frantisek HANACEK and Vladimir VASINEK. Optical fiber distributed temperature sensor in cardiological surgeries. In: *Proceedings of SPIE - The International Society for Optical Engineering*. Bellingham: SPIE, 2010, pp. 312-318. ISBN 978-081948199-3. DOI: 10.1117/12.854309.

About Authors

Petr KOUDELKA was born in 1984 in Prostejov. In 2006, he finished bachelor study at VSB-Technical University of Ostrava, Faculty of Electrical Engineering and Computer Science, Dept. of Electronic and Telecommunications. Two years later, he finished M.Sc. in the field of optoelectronics. In the present time during his Ph.D. study he is interested in VLC (*Visible Light Communication)*, Distributed Temperature Sensing systems and optical technologies PON (*Passive Optical Networks*).

Jan LATAL was born in 1983 in Prostejov. He received his B.Sc. Degree from the VSB-Technical University of Ostrava, Faculty of Electrical Engineering and Computer Science, Dept. of Electronic and Telecommunications in 2006. He received his M.Sc. Degree from the Technical University of Ostrava, Faculty of Electrical Engineering and Computer Science, Dept. of Telecommunications in 2008. Currently in doctor degree studies, he focuses on optical technologies (xPON) and especially on free space optics, fiber optics sensors etc. He is a member of SPIE and IEEE.

Jan VITASEK was born in 1984 in Opava. In 2009 he finished M.Sc. study at Brno University of Technology, Faculty of Electrical Engineering and Communication. In present time he is Ph.D. student at VSB−Technical University of Ostrava. His interests are propagation and processing of optic signals.

Petr SISKA was born in 1979 in Kromeriz. In 2005 he finished M.Sc. study at VSB-Technical University of Ostrava, Faculty of Electrical Engineering and Computer Science, Dept. of Electronic and Telecommunications. Three years later, he finished Ph.D. study in Telecommunication technologies. Currently he is employee of Department of Telecommunications. He is interested in Optical communications, Fiber optic sensors and Distributed Temperature Sensing systems.

Andrej LINER was born in 1987 in Zlate Moravce. In 2009 received Bachelor's degree on University of Zilina, Faculty of Electrical Engineering, Department of Telecommunications and Multimedia. Two years later he received on the same workplace his Master's degree in the field of Telecommunications and Radio Communications Engineering. He is currently Ph.D. student, and he works in the field of wireless optical communications and fiber optic distributed systems.

Martin PAPES was born in 1987 in Nove Zamky. In 2009 received Bachelor's degree on University of Zilina, Faculty of Electrical Engineering, Department of Telecommunications and Multimedia. Two years later he received on the same workplace his Master's degree in the field of Telecommunications and Radio Communications Engineering. He is currently Ph.D. student, and he works in the field of wireless optical communications and fiber optic distributed systems.